A Fundamental Model for Continuous Intraday Electricity Trading

Marcel Kremer[*a], Rüdiger Kiesel[a,b], and Florentina Paraschiv[c,d]

[a]*Chair for Energy Trading and Finance, University of Duisburg-Essen, Universitätsstraße 12, 45141 Essen, Germany*
[b]*Department of Mathematics, University of Oslo, PO Box 1053 Blindern, 0316 Oslo, Norway*
[c]*NTNU Business School, Norwegian University of Science and Technology, 7491 Trondheim, Norway*
[d]*Institute for Operations Research and Computational Finance, University of St. Gallen, Bodanstrasse 6, CH-9000 St. Gallen, Switzerland*

November 29, 2019

Abstract

This paper develops a fundamental price model for continuous intraday electricity markets of 15-minute contracts. A unique data set of intradaily updated forecasts of renewable power generation is analyzed. We use a threshold regression model to examine how 15-minute intraday trading depends on the slope of the merit order curve. Our estimation results reveal strong evidence of mean reversion in the price formation mechanism of 15-minute contracts. Additionally, prices of neighboring contracts exhibit strong explanatory power and a positive impact on prices of a given contract. We observe an asymmetric effect of renewable forecast changes on intraday prices depending on the merit-order-curve slope. In general, renewable forecasts have a higher explanatory power at noon than in the morning and evening, but price information is the main driver of 15-minute intraday trading.

Keywords: Continuous intraday electricity market; Fundamental model; 15-minute contracts; Renewable power forecasts; Merit order curve; Threshold regression

JEL Classification: C22; C24; C55; G10; Q20; Q21; Q40; Q41; Q42

1 Introduction

In recent years, the expansion of renewable energy sources has been forged ahead massively across the globe with a direct impact on electricity markets. As electricity generation from renewable energy sources cannot be predicted reliably in the long-term, that is, days, weeks or months ahead, the future of electricity trading is foreseen in short-term electricity markets. Energy supply companies thus face the challenge of moving towards automatic trading, which requires the identification of trading strategies based on local demand and supply patterns as well as cross-border energy flows. The German market constitutes a pioneer among European

---

[*]Corresponding author. Email: marcel.kremer@uni-due.de

electricity markets. Not only is the German market the largest electricity market in Europe in terms of total trading volume (European Energy Exchange AG, 2016a), but also novel developments and innovations (new contracts, reduction of lead time) are traditionally introduced on the German market first. In Germany the most short-term electricity market is the continuous intraday market, where hourly and 15-minute contracts can be traded until 30 minutes before the delivery of electricity begins. Intraday electricity markets are designed according to the needs of energy supply companies to balance forecast errors of renewable power generation.

This paper investigates four research questions: (i) Which fundamental factors drive the continuous intraday trading of 15-minute contracts? (ii) How do forecast changes of renewable power generation affect the intraday trading of 15-minute contracts? (iii) Can we identify different regimes on the intraday market where the price formation process behaves differently? (iv) How does intraday trading depend on the time of day?

Like on any financial market, there is a natural desire for pricing models of the fundamental securities. To build as realistic models as possible, we require *ex-ante* information on the underlying price drivers. More market-specifically, and in light of the design of intraday electricity markets, forecast errors of renewable power production have to be taken into account. Kiesel and Paraschiv (2017) deliver the first and only work fulfilling these prerequisites. Our article builds upon their work and develops a fundamental price model for continuous intraday markets of 15-minute contracts.

Our main modeling assumption is that the price formation process on the intraday electricity market depends on the slope of the merit order curve. Figure 1 illustrates a merit order curve with and without the infeed from renewable energy sources (RES). The merit order curve is a non-linear and convex function of the marginal costs of power plants depending on the generation capacity. Equivalently, since the marginal costs of the last running power plant needed to cover demand set the final electricity price, the merit order curve may be interpreted as a function of the electricity price depending on the electricity demand, too.

Let us consider the merit order curve without renewable power infeed (blue solid). When there is low demand, only relatively cheap power generation technologies such as lignite-fired power plants are needed, whereas if demand is high, more expensive technologies such as gas-fired power plants might be required to satisfy demand. As exhibited in Figure 1, if demand is low, the slope of the merit order curve is relatively small and we call the market to be in a flat merit-order regime; however, if demand is high, the merit-order-curve slope is comparatively large and the market is said to be in a steep merit-order regime.

Let us turn towards the merit order curve with renewable power infeed (green dash-dotted). Since renewable energy sources have zero marginal costs, their infeed shifts the entire merit order curve to the right. As a consequence, if demand is low (flat regime), the electricity price decreases by a small amount ΔP_f; however, if demand is high (steep regime), the electricity price decreases as well but by a much larger amount $\Delta P_s > \Delta P_f$. We take into account this asymmetric effect of renewable power infeed on electricity prices in our fundamental model by incorporating the slope of the merit order curve.

To model the merit order curve, two approaches have been proposed in the academic literature. The first approach models the merit order curve from the supply side via generation capacities and marginal costs of power plants. While generation capacities are given by market transparency data, one has to specify a model for the marginal costs of power plants. Pape et al. (2016) model the marginal costs as a function of fuel prices, CO_2 emission allowances prices, emission intensities per fuel type, power plant heat rates, and other variable costs. As marginal costs depend on a wide variety of factors, this approach is highly complex and subject to strong modeling assumptions. The second approach models the merit order curve from the demand side via electricity loads, or load forecasts, and electricity prices as proposed by Burger et al. (2004); He et al. (2013). While electricity load is an indicator of total electricity demand, electricity prices are determined by the marginal costs of the price-setting power plant (marginal
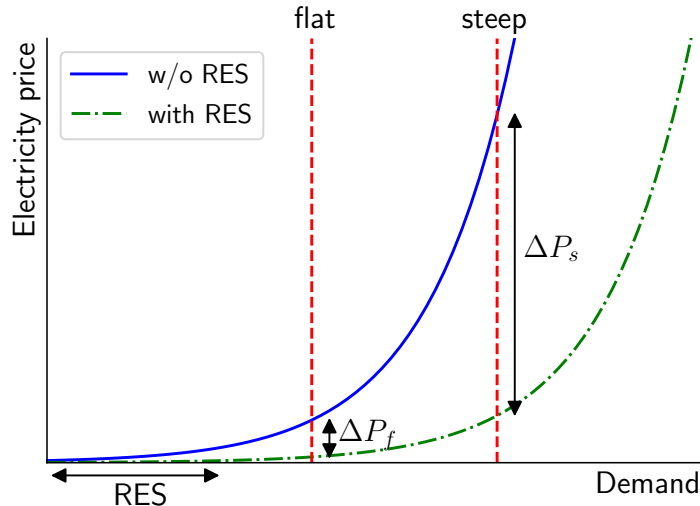
Figure 1: Merit order curve without (blue solid) and with (green dash-dotted) infeed from renewable energy sources (RES) indicating a flat and steep merit-order regime (red) with electricity price changes ΔP_f and ΔP_s, respectively.

power plant). As data for both electricity loads and prices exist, this approach does not rely on modeling assumptions. Therefore we follow the demand-side approach.

The continuous intraday electricity market of 15-minute contracts has only recently come into focus of scientific research. To the best of our knowledge, only three studies exist hitherto. Kiesel and Paraschiv (2017) provide the first econometric analysis and fundamental model for 15-minute intraday prices. They model both deviations between day-ahead and last intraday prices as well as continuous intraday prices in a threshold regression context. They provide evidence that 15-minute prices react asymmetrically to intradaily updated renewable forecast errors depending on the proportion of expected demand covered by conventional energy sources. Märkle-Huß et al. (2018) study how the introduction of 15-minute contracts has affected the day-ahead and intraday market of hourly contracts. They find that prices of hourly contracts decreased and trading volumes increased. Kath and Ziel (2018) present the first forecasting study of 15-minute prices using an elastic net regression model. They conclude that prices in the intraday auction are much easier to forecast than prices in the continuous trading.

This article extends the existing literature along a number of dimensions: First, we explore a novel and unique data set of high-frequency transaction data and linked fundamental supply and demand data. Intradaily updated forecasts of renewable power generation (solar, wind) constitute the heart of our data collection. These are the same real-time renewable forecasts as available to traders on the intraday market. As such this is the most extensive data set used in the empirical literature to study the price formation process on intraday electricity markets. Hence our data set allows for a more realistic model specification than proposed in previous research.

Second, we suggest the first fundamental price model for 15-minute contracts that incorporates the slope of the merit order curve. This is a substantial improvement over Kiesel and Paraschiv (2017) as electricity prices react asymmetrically to renewable forecast changes depending on the merit-order-curve slope: If the merit order is steep, electricity prices change more severely in the wake of renewable forecast errors than if the merit order is flat. Moreover, our fundamental model solely involves *ex-ante* market knowledge.

Third, and to the best of our knowledge, this is the first work studying the influence of neighboring 15-minute contracts on the price dynamics of a given contract. This is motivated

by the fact that adjacent contracts are driven by similar market information.

This paper is organized as follows: In Section 2 we lay out our data set and perform an empirical analysis of intraday transaction data of 15-minute contracts. In Section 3 we present the existing fundamental model by Kiesel and Paraschiv (2017) and our extended version of the model as well as the threshold regression. In Section 4 we calibrate the fundamental models to market data and discuss our estimation results. We offer our conclusions in Section 5.

2 Stylized facts of the intraday market

In this section we lay out our data set and empirically analyze transaction prices and trading volumes of 15-minute contracts.

2.1 Data

We investigate high-frequency trade and linked fundamental data of all 96 15-minute contracts traded on the German continuous intraday power market at EPEX SPOT SE. Our observation period spans from January 1 to December 31, 2015. The trade data of 15-minute contracts involve transaction prices and trading volumes from the continuous intraday trading session with a 1-minute time resolution and are provided by European Energy Exchange AG (2016c). The continuous trading session for 15-minute contract opens daily at 4 PM and ends 45 and 30 minutes before delivery begins, respectively[1]. Furthermore, we use market clearing prices of 15-minute contracts traded in the German 15-minute intraday auction at EPEX SPOT SE, which takes place daily at 3 PM, provided by European Energy Exchange AG (2016b). The auction data may also be obtained via the R package `emarketcrawlR` by Wagner (2018).

As fundamental data, we include intraday wind and solar power forecasts, expected demand and expected conventional capacity. The intraday renewable power forecasts involve intradaily updated forecasts of wind and solar power production in Germany, which are the same real-time renewable forecasts as available to traders on the intraday market. These forecasts are updated every 15 minutes, where each update contains a forecast time series for the following eight days in a 15-minute time resolution, provided by EWE TRADING GmbH (2016). As such the intraday renewable power forecasts constitute a unique data set and, to the best of our knowledge, have solely been analyzed by Kiesel and Paraschiv (2017). As an indicator of expected electricity demand, we use the day-ahead total load forecast for each quarter-hour on the following day in Germany, which is published daily at 10 AM and is provided European Network of Transmission System Operators for Electricity Transparency Platform (2016). The expected conventional capacity covers the expected daily average of available generation capacity of conventional power plants on the following day in Germany, which is published daily at 10 AM and is provided by European Energy Exchange AG Transparency Platform (2016). As conventional energy sources, we include coal, garbage, gas, lignite, oil, other, pumped-storage, run-of-the-river, seasonal-store, uranium. A summary of the employed data may be found in Table 8 in Appendix A.

2.2 Hourly seasonality

2.2.1 Transaction prices

Figure 2 illustrates the mean transaction price of 15-minute contracts during peak hours and off-peak hours for summer and winter. We identify an hourly seasonality of mean transaction prices for both peak and off-peak hours as well as for summer and winter. The hourly seasonality exhibits a sawtooth-like shape: For the peak-hour contracts H8Q1–H13Q4, the mean price of

---

[1]EPEX SPOT SE reduced the lead time on the German continuous intraday power market for hourly and 15-minute contracts from 45 to 30 minutes before delivery on July 16, 2015 (EPEX SPOT SE, 2015).

the first 15-minute contract within each hour is the highest and it declines until the last 15-minute contract within that hour, which has the lowest mean price. Conversely, for contracts H14Q1–H18Q4, the lowest mean price is present for the first 15-minute contract which increases up to the highest mean price for the last 15-minute contract in a given hour.

The hourly seasonality pattern and its change around noon may be explained by electricity generation from solar energy: In the first half of the day, the sun rises and less electricity from solar energy is produced during the first quarter-hour as compared to the last quarter-hour within each hour. If a (renewable) electricity supplier sold an hourly contract on the day-ahead market, it has to buy electricity for the first quarter-hour on the intraday market to meet its obligation since less electricity is produced from solar energy than it has sold (buy pressure); thus prices increase. In the last quarter-hour, however, more solar electricity is generated than it has sold on the day-ahead market and so it wants to sell the surplus on the intraday market to avoid entering the balancing energy market (sell pressure); hence prices decrease. In the second half of the day, after the sun has reached its highest level (around 2 PM in Germany), more solar power is generated during the first than in the last quarter-hour in each hour. Thus there is a sell pressure in the first and a buy pressure in the last quarter-hour of an hour, and the pattern is reversed. The existence of buy and sell pressure is underpinned by the hourly seasonality of trading volumes described in Section 2.2.2.

Similarly the sawtooth-shaped hourly seasonality of mean transaction prices is found during off-peak hours. For contracts H20Q1–H1Q4, the mean price of the first and last quarter-hourly contract within an hour is highest and lowest, respectively, while for contracts H4Q1–H6Q4, this is reversed. The hourly seasonality at night stems from the design of conventional power plants which ramp up and down.

Overall during peak hours, mean transaction prices are lower in summer than in winter apart from a few exceptions. In the afternoon and evening hours, that is, for contracts H14Q1–H19Q4, we find larger deviations between summer and winter mean prices than in morning and noon hours. During off-peak hours, mean prices are fairly similar during both seasons most of the time and only slightly lower in winter than in summer.
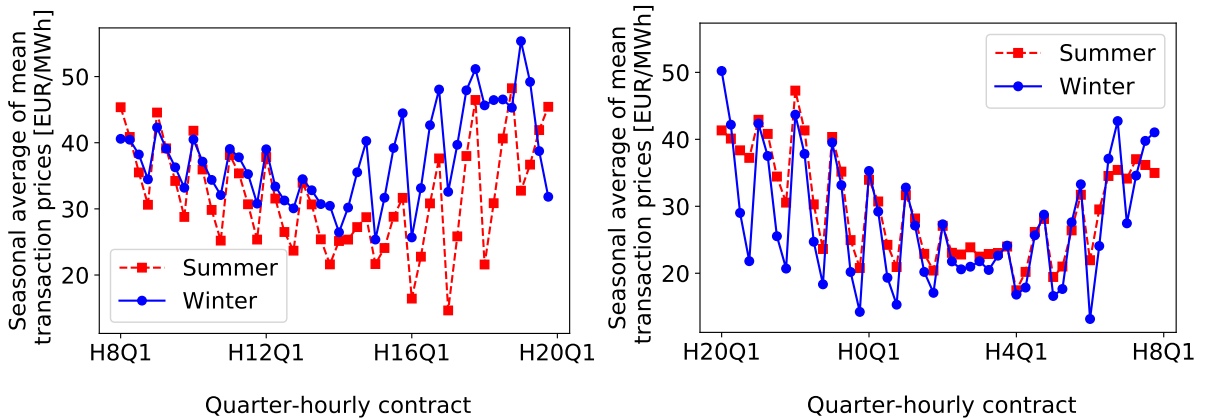
Figure 2: Mean transaction price of 15-minute contracts during peak hours (left) and off-peak hours (right) averaged over summer (red) and winter (blue).

2.2.2 Trading volumes

Figure 3 shows the total trading volume of 15-minute contracts during peak hours and off-peak hours averaged over the year. We only present the yearly average of total trading volumes as the distinction between summer and winter does not provide additional information. Similar to transaction prices, we observe an hourly seasonality of total trading volumes for both peak and off-peak hours. The hourly seasonality of trading volumes has a U-shape: Larger total

trading volumes are found for the first and last 15-minute contract within each hour of the day, while the second and third 15-minute contract in an hour always exhibit lower trading volumes. More specifically, the last 15-minute contract entails the largest trading volume, while the second 15-minute contract involves the lowest trading volume in an hour. The U-shaped hourly seasonality supports our hypothesis of buy and sell pressure for the marketing of solar power in the first and last quarter-hour during peak hours, respectively.

15-minute contracts during off-peak hours are generally associated with less trading volume than peak-hour contracts. Total trading volumes are particularly low for contracts H0Q1–H5Q4. However, the U-shaped hourly seasonality of trading volumes is persistent during off-peak hours. The hourly seasonality at night results from balancing out the ramp-up and -down of conventional power plants.
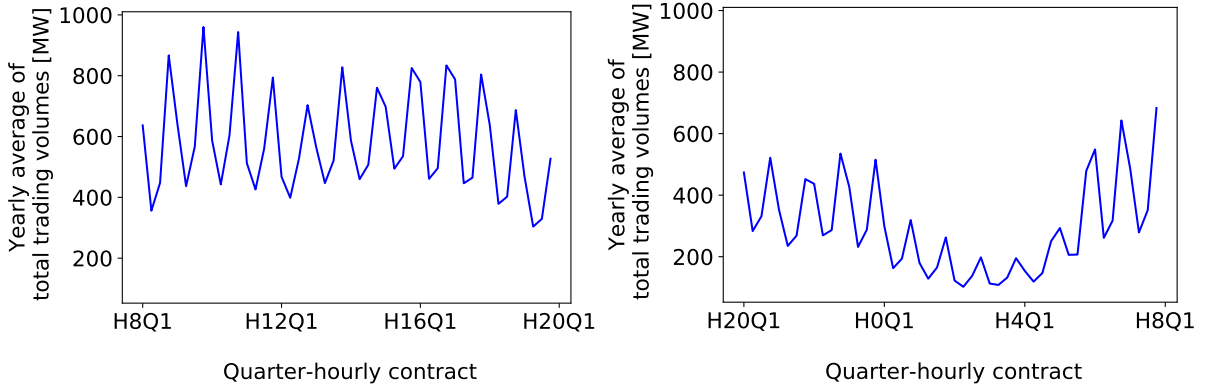
Figure 3: Total trading volume of 15-minute contracts during peak hours (left) and off-peak hours (right) averaged over the year.

2.3 Liquidity evolution

Figure 4 displays the temporal evolution of liquidity of 15-minute contracts over the trading session towards gate closure. As measures for liquidity, we use the number of trades and total trading volume aggregated over all 15-minute contracts and all trading sessions. Due to low liquidity far from gate closure, we focus on the last three trading hours prior to gate closure. We note that EPEX SPOT SE reduced the lead time on the German continuous intraday power market for hourly and 15-minute contracts from 45 to 30 minutes before delivery on July 16, 2015 (EPEX SPOT SE, 2015)[2]. Thus to avoid effects due to the shift of lead time, we synchronize our trade time series with respect to gate closure by shifting the trade time stamps of 15-minute contracts maturing before July 16, 2015 by 15 minutes.

The number of trades increases from 952 three hours to gate closure to 3,054 one hour to gate closure. Subsequently the number of trades rises further and more than doubles to 7,080 half an hour to gate closure. 15 minutes to gate closure, the number of trades jumps to 16,593 while 13 minutes before gate closure it reaches a local maximum of 28,378. The surge of trading activity around 15 minutes to gate closure may be associated with the fact that a given contract becomes the front 15-minute contract. The maximum value of 30,512 trades is observed one minute to gate closure.

The total trading volume increases from 12 GW to 48 GW between three and one hour to gate closure. Thereafter trading volume almost triples to 135 GW half an hour to gate closure. 15 and 13 minutes before gate closure, total trading volume raises to 261 GW and 314 GW, respectively, which coincides with becoming the front 15-minute contract. A comparison with

---

[2]On June 14, 2017, the lead time within the four German control zones was locally further reduced to 5 minutes before delivery (EPEX SPOT SE, 2017).

the number of trades at these points in time in Figure 4 reveals that indeed a vast number of transactions are executed but with comparatively low trading volumes. The total trading volume peaks at 960 GW one minute to gate closure.

Thus we observe that liquidity of 15-minute contracts rises severely within the last trading hour prior to gate closure: On average, roughly 68% of the number of transactions are executed and roughly 74% of the total trading volume is transferred. The reason why the majority of trading takes place close to gate closure is that forecasts of fundamentals, particularly renewable power forecasts, become more and more precise regarding the delivery period of a given 15-minute contract. Hence it is desirable to trade as closest to delivery begin as possible.

We identify a small but distinct rise in liquidity every 15 minutes. This is particularly pronounced for the number of trades but present for the total trading volume, too. Consequently, an increased amount of transactions with relatively little trading volume is conducted periodically. We argue that the 15-minute periodicity in liquidity originates from newly arriving renewable forecast updates. As described in Section 2.1, renewable forecasts are updated in 15-minute intervals. New forecasts will not have changed much after 15 minutes and thus traders only make minor adjustments to their positions by trading little volume. Moreover, we observe that trading activity increases at isolated points in time and dies out immediately until the next increase. Therefore we conclude that renewable forecast updates are reflected in prices of 15-minute contracts within one trading minute.
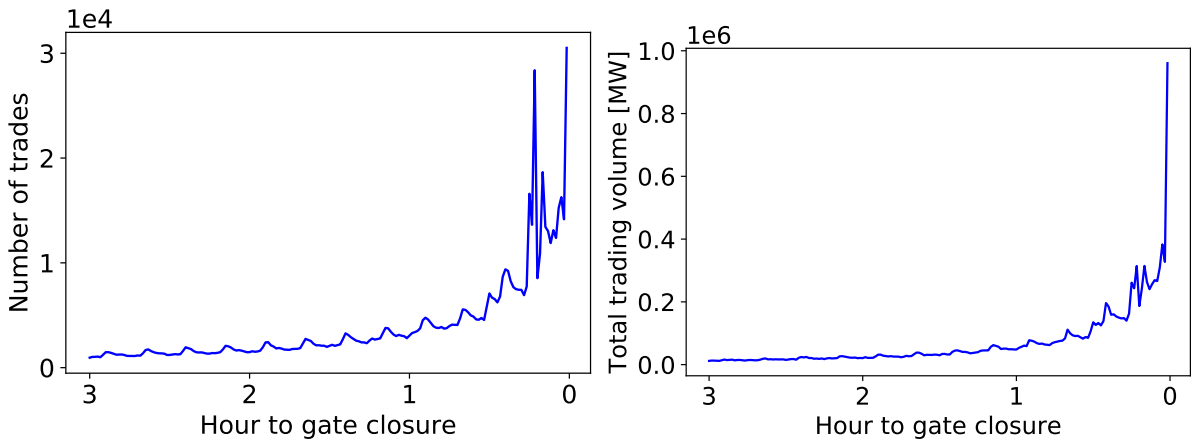
Figure 4: Time evolution of the number of trades (left) and total trading volume (right) through the trading session towards gate closure.

3 Methodology

We aim at modeling the asymmetric behavior of 15-minute intraday electricity prices to explanatory variables, in particular, to renewable forecast changes. As a starting point, we reimplement the fundamental model by Kiesel and Paraschiv (2017). Moreover, we suggest an extension of their model to overcome its weaknesses. We employ a threshold regression model to calibrate the fundamental models to market data.

3.1 Benchmark fundamental model

As a benchmark, we employ the fundamental model for continuous intraday price changes of 15-minute contracts proposed by Kiesel and Paraschiv (2017). For each 15-minute contract, the

model specification reads

$$\Delta P_t = \alpha_0 + \sum_{\tau=1}^{3} \alpha_\tau \, \Delta P_{t-\tau} + \alpha_4 \, V_t + \alpha_5 \, DQ + \alpha_6 \, \Delta w_t^n + \alpha_7 \, \Delta w_t^p$$
$$+ \alpha_8 \, \Delta s_t^n + \alpha_9 \, \Delta s_t^p + \alpha_{10} \, \sqrt{\Delta t} + \epsilon_t \,, \tag{1}$$

where $\Delta P_t = P_t - P_{t-1}$ denotes the transaction price change between times t and $t-1$, V_t the trading volume at time t, $DQ = \frac{\ell}{c}$ the demand quota with expected demand ℓ and expected conventional capacity c for a given 15-minute contract, $\Delta w_t^n = \min(\Delta w_t, 0)$ and $\Delta w_t^p = \max(\Delta w_t, 0)$ negative and positive wind power forecast changes, respectively, where $\Delta w_t = w_t - w_{t-1}$ is the wind power forecast change between times t and $t-1$, $\Delta s_t^n = \min(\Delta s_t, 0)$ and $\Delta s_t^p = \max(\Delta s_t, 0)$ negative and positive solar power forecast changes, respectively, where $\Delta s_t = s_t - s_{t-1}$ is the solar power forecast change between times t and $t-1$, and Δt the interarrival time between two consecutive transactions conducted at times t and $t-1$.

The demand quota DQ quantifies the proportion of expected demand which is expected to be met by conventional power generation capacities, or, put another way, how much the expected conventional capacity does cover expected demand. DQ is the only variable remaining constant during the continuous trading session of a given 15-minute contract. However, it does depend on the specific contract since the expected demand l is provided in quarter-hourly granularity. In particular, the value of the demand quota is known daily at 10 AM and thus before continuous trading begins. We use DQ as threshold variable since we assume that the gap between expected demand and expected conventional capacity influences the trading behavior of market participants on the intraday market: A large gap induces a great necessity to balance electricity produced from renewable energy sources, whereas a small gap puts less pressure to adjust renewable electricity (see Kiesel and Paraschiv, 2017, chap. 2, for a more detailed discussion). From a trader's perspective, the demand quota is well suited as threshold variable, too, since it indicates in which regime the market is before continuous trading begins. Thereby the corresponding intraday price model can be chosen *ex-ante*.

The sum in Equation (1) covers three lagged price changes $\Delta P_{t-\tau}$, $\tau = 1, \ldots, 3$, that is, autoregressive terms, where the number of lags has been determined by partial autocorrelation of price changes. Moreover, we distinguish between positive and negative wind and solar power forecast errors $\Delta w_t^p, \Delta s_t^p$ and $\Delta w_t^n, \Delta s_t^n$, respectively, as we expect them to have a different effect on the electricity price change ΔP_t: A positive renewable forecast error should decrease the electricity price, whereas a negative renewable forecast error should increase the electricity price. We control for the interarrival time Δt since transactions do not take place at equidistant points in time, but it may take one minute or several hours until the next trade is conducted.

3.2 Extended fundamental model

In Kiesel and Paraschiv (2017), one weakness of the demand quota is that it does not recognize whether the market is in a flat or steep merit-order-curve regime: Proportionally speaking, a high expected demand and high expected conventional capacity lead to the same value of DQ as low demand and low capacity. Another weakness is that the demand quota aggregates expected capacities over all conventional generation technologies. Thus it loses information on the price-setting power plant and the slope of the merit order curve. We overcome these limitations in our extended version of the model.

We refine the fundamental model by Kiesel and Paraschiv (2017) along three dimensions by incorporating supplementarily: (i) the slope of the merit order curve, (ii) price changes of neighboring 15-minute contracts, (iii) the 15-minute intraday auction price. For a given

15-minute contract $i = 1, \ldots, 96$, the model specification reads

$$\Delta P_t^{(i)} = \alpha_0^{(i)} + \sum_{\tau=1}^{m} \alpha_\tau^{(i)} \Delta P_{t-\tau}^{(i)} + \sum_{\substack{j=-n, \\ j \neq 0}}^{n} \beta_j^{(i)} \Delta P_t^{(i+j)} + \eta_1^{(i)} \xi^{(i)} + \eta_2^{(i)} P^{\mathrm{Auc},(i)} + \eta_3^{(i)} V_t^{(i)}$$
$$+ \eta_4^{(i)} \Delta w_t^{n,(i)} + \eta_5^{(i)} \Delta w_t^{p,(i)} + \eta_6^{(i)} \Delta s_t^{n,(i)} + \eta_7^{(i)} \Delta s_t^{p,(i)} + \eta_8^{(i)} \sqrt{\Delta t^{(i)}} + \epsilon_t^{(i)}, \qquad (2)$$

where $\xi^{(i)}$ denotes the slope of the merit order curve of contract i, and $P^{\mathrm{Auc},(i)}$ the 15-minute intraday auction price of contract i. The remaining variables correspond to the benchmark model (1) described in Section 3.1. $\xi^{(i)}$ and $P^{\mathrm{Auc},(i)}$ are the only variables remaining constant during the trading session of contract i. We use the slope of the merit order curve $\xi^{(i)}$ as threshold variable instead of the demand quota. The value of $\xi^{(i)}$ can be determined daily at 10 AM and hence before continuous trading begins. Thereby we know whether the market is in a flat or steep merit-order regime *ex-ante* and the appropriate intraday price model can be chosen accordingly. This is an attractive feature of our fundamental model for practical applications.

We estimate $\xi^{(i)}$ from empirical intraday auction prices $P^{\mathrm{Auc},(i)}$ and expected demands $\ell^{(i)}$ in the spirit of Burger et al. (2004); He et al. (2013). This approach is reasonable for describing the slope of the merit order curve since the level of intraday auction prices reflects the marginal costs of power plants needed to cover expected demand. They construct a merit order curve for the electricity spot market as a whole, independent of the contract, from hourly day-ahead prices and hourly load forecasts. We, however, determine a merit order curve for each 15-minute contract i individually and thus arrive at a more fine-grained picture. We fit a function $f(\ell)$ to the price-load data and call $f(\ell)$ the empirical merit order curve[3]. Then we take the derivative of the empirical merit order curve $f'(\ell) = \frac{\mathrm{d}f(\ell)}{\mathrm{d}\ell}$ and substitute empirical expected demands $\ell^{(i)}$ into $f'(\ell)$ to obtain empirical merit-order-curve slopes $\xi^{(i)} = f'(\ell^{(i)})$.

The second sum in Equation (2) captures the price change ΔP_t between times t and $t - 1$ of n 15-minute contracts maturing before and n 15-minute contracts maturing after contract i. For example, if $n = 2$ and $i = \mathrm{H13Q1}$, the price change at time t of contracts H12Q3, H12Q4, H13Q2, H13Q3 is included. The intraday auction price $P^{\mathrm{Auc},(i)}$ is determined daily at 3 PM and can be considered as an estimate of the initial price of a 15-minute contract i in the continuous trading session.

3.3 Threshold regression

We use the threshold regression model introduced by Hansen (2000) to calibrate our fundamental models to market data. The threshold regression model is able to reveal asymmetries in the impact of explanatory variables with respect to a specified threshold variable. The basic concept of the threshold regression involves two steps: First, we split the entire sample into two subsamples, also referred to as groups, classes, or regimes; second, we estimate a linear regression model on each subsample separately.

More formally, suppose we observe the sample $\{y_i, \mathbf{x}_i, q_i\}_{i=1}^n$, where y_i is the dependent variable, $\mathbf{x}_i \in \mathbb{R}^m$ an m-vector collecting the independent variables, and q_i the threshold variable. The threshold variable q_i may be one of the independent variables gathered in $\mathbf{x}_i$ and must have a continuous distribution. The threshold regression model reads

$$y_i = \begin{cases} \boldsymbol{\theta}_1' \mathbf{x}_i + \varepsilon_i, & \text{if } q_i \leq \gamma \\ \boldsymbol{\theta}_2' \mathbf{x}_i + \varepsilon_i, & \text{if } q_i > \gamma \end{cases},$$
$$= \boldsymbol{\theta}_1' \mathbf{x}_i \mathbb{1}\{q_i \leq \gamma\} + \boldsymbol{\theta}_2' \mathbf{x}_i \mathbb{1}\{q_i > \gamma\} + \varepsilon_i, \qquad i = 1, \ldots, n, \qquad (3)$$

where γ is the threshold parameter, $\boldsymbol{\theta}_1, \boldsymbol{\theta}_2 \in \mathbb{R}^m$ the regression parameters, and ε_i the error term. Thus the observed sample is split into two subsamples along the threshold variable q_i at a

---

[3]Burger et al. (2004) call f empirical price load curve.

specific value γ. By design, the threshold regression model (3) allows the regression parameters $\boldsymbol{\theta}_1, \boldsymbol{\theta}_2$ to vary between the regimes.

We define $\mathbf{x}_i(\gamma) = \mathbf{x}_i \, \mathbb{1}\{q_i \leq \gamma\}$, where $\mathbb{1}$ denotes the indicator function, and call $\boldsymbol{\delta}_n = \boldsymbol{\theta}_1 - \boldsymbol{\theta}_2$ the threshold effect. Then we can write the threshold regression model (3) in the alternative form

$$y_i = \boldsymbol{\theta}' \mathbf{x}_i + \boldsymbol{\delta}_n' \, \mathbf{x}_i(\gamma) + \varepsilon_i, \qquad i = 1, \dots, n, \tag{4}$$

where $\boldsymbol{\theta} = \boldsymbol{\theta}_2$. Stacking the variables y_i and ϵ_i results in n-vectors $\mathbf{y}, \boldsymbol{\varepsilon} \in \mathbb{R}^n$, and stacking the vectors $\mathbf{x}_i'$ and $\mathbf{x}_i(\gamma)'$ yields $n \times m$ matrices $\mathbf{X}, \mathbf{X}_\gamma \in \mathbb{R}^{n \times m}$. Then we can rewrite Equation (4) in matrix notation

$$\mathbf{y} = \mathbf{X}\,\boldsymbol{\theta} + \mathbf{X}_\gamma\,\boldsymbol{\delta}_n + \boldsymbol{\varepsilon}, \tag{5}$$

where $(\boldsymbol{\theta}, \boldsymbol{\delta}_n, \gamma)$ are the regression parameters which can be estimated by least squares (LS). By definition, the LS estimators $\hat{\theta}, \hat{\delta}, \hat{\gamma}$ jointly minimize the sum of squared errors function

$$S_n(\theta, \delta, \gamma) = (\mathbf{Y} - \mathbf{X}\,\boldsymbol{\theta} - \mathbf{X}_\gamma\,\boldsymbol{\delta})' \, (\mathbf{Y} - \mathbf{X}\,\boldsymbol{\theta} - \mathbf{X}_\gamma\,\boldsymbol{\delta}). \tag{6}$$

Following the derivation by Hansen (2000), the threshold parameter estimate $\hat{\gamma}$ is the value that minimizes the concentrated sum of squared errors function

$$S_n(\gamma) = \mathbf{Y}'\mathbf{Y} - \mathbf{Y}'\mathbf{X}_\gamma^* \, (\mathbf{X}_\gamma^{*\prime}\mathbf{X}_\gamma^*)^{-1}\mathbf{X}_\gamma^{*\prime}\, \mathbf{Y}, \tag{7}$$

where $\mathbf{X}_\gamma^* = [\mathbf{X}\,\mathbf{X}_\gamma]$, that is,

$$\hat{\gamma} = \arg\min S_n(\gamma). \tag{8}$$

To test the hypothesis $H_0 : \gamma = \gamma_0$, a standard approach is to use the likelihood ratio statistic

$$LR_n(\gamma) = n\,\frac{S_n(\gamma) - S_n(\hat{\gamma})}{S_n(\hat{\gamma})}, \tag{9}$$

under the auxiliary assumption $\varepsilon_i \overset{\text{iid}}{\sim} \mathcal{N}(0, \sigma^2)$. The likelihood ratio test of H_0 is to reject for large values of $LR_n(\gamma_0)$. We can calculate asymptotic p-values for the likelihood ratio test by

$$p_n = 1 - \left(1 - \mathrm{e}^{-\frac{1}{2}\,LR_n(\gamma_0)^2}\right)^2. \tag{10}$$

4 Estimation results

4.1 Benchmark fundamental model

We estimate the coefficients of the benchmark fundamental model (1) by Kiesel and Paraschiv (2017) by the threshold regression described in Section 3.3 for all 96 15-minute contracts. Here a selection of 15-minute contracts representative for morning, noon, and evening hours is analyzed, that is, H7, H13, H18, Q1–Q4 each. Our estimation results stemming from January–December 2015 data are compared with the results by Kiesel and Paraschiv (2017), who study January–June 2014 data. For all contracts, we use the demand quota DQ as threshold variable.

The estimation results of all 15-minute contracts in hours H13, H7, H18 are presented in Tables 1, 2, 3, respectively. The threshold parameter estimate is highly statistically significant and amounts to $\hat{\gamma} \approx 1.1$ for all contracts in hours H13 and H7, while in hour H18, it is only statistically significant for contract Q2. A demand quota of $DQ = 1.1$ implies that the expected total electricity demand exceeds expected conventional capacity by approximately 10%. Likewise this value implies that roughly 10% renewable power infeed is expected. In

general, the low demand quota regime (Regime 1) describes a market in which much conventional power generation is planned to meet expected demand, since little renewable power production is anticipated. Conversely, the market is in the high demand quota regime (Regime 2) if much renewable power infeed is anticipated and consequently less conventional power generation is planned. For all contracts, the total sample is split into subsamples of reasonable size and allows for a sound interpretation of the estimation results. The adjusted R^2 ranges between 9% and 23%.

The estimated coefficients of the lagged price changes $\Delta P_{t-1}, \Delta P_{t-2}$ are highly statistically significant and negative in both regimes for all contracts, and even the coefficients of ΔP_{t-3} are significant and negative in most cases. For evening contracts, the higher-order autoregressive terms lose statistical significance. The negative coefficients of lagged price changes are an indicator of mean reversion in the price formation process of 15-minute contracts. As such they reflect the so-called "learning effect" or "participant conduct" (Karakatsani and Bunn, 2010; Frauendorfer et al., 2018). Our results confirm previous findings of Kiesel and Paraschiv (2017) for morning and evening contracts. For noon contracts, in contrast, they find that autoregressive terms are less significant and trading is primarily driven by renewable forecast changes. Our results, however, suggest that autoregressive terms and the mean reversion pattern associated therewith play an essential role at noon in 2015.

The estimated coefficients of trading volume V_t are statistically significant for most of the contracts and regimes. For contracts H13Q1 and H13Q2 they are negative, whereas for H13Q3 and H13Q4 they turn positive independent of the regime. The same sign profile is found for contracts H18Q1 and H18Q4. This sign pattern is reasonable as it reflects the joint hourly seasonality of transaction prices and trading volumes described in Section 2.2: In the first and second half of an hour, more and less solar power is produced than the hourly average which induces sell and buy pressure, respectively. Consequently, electricity prices decrease and increase in the first and last quarter-hours of an hour. In morning hours, we observe the opposite: For contracts H7Q1 and H7Q2 the coefficients of V_t are positive, whereas for H7Q3 and H7Q4 they turn negative independent of the regime. This sign pattern coincides with buy and sell pressure at the beginning and end of the hour, respectively. Overall, we find an asymmetric adjustment of intraday price changes ΔP_t to trading volumes V_t. This confirms the results of Kiesel and Paraschiv (2017).

In hour H13, the coefficients of negative wind forecast changes Δw_t^n are statistically significant and negative in both regimes for all contracts, whereas coefficients of positive wind forecast changes Δw_t^p are not significant. In Kiesel and Paraschiv (2017), the coefficients of Δw_t^n are also negative but only significant for some contracts. In hour H7, the coefficients of negative wind forecast changes Δw_t^n are significant and negative in the high demand quota regime for Q1–Q3, whereas coefficients of positive wind forecast changes Δw_t^p are significant and negative for Q1 and Q2. In Kiesel and Paraschiv (2017), the coefficients of Δw_t^n are also not significant, while some coefficients of Δw_t^p are significant but with no clear regularity. In hour H18, the coefficients of negative and positive wind forecast changes $\Delta w_t^n, \Delta w_t^p$ are rarely significant and mostly negative. Overall, no asymmetry in the coefficients of wind forecast changes between the regimes is found. We conclude that forecast errors of wind power generation contribute to pricing electricity for noon contracts, but they are less significant for pricing morning and evening contracts.

In hours H13 and H7, the coefficients of negative solar forecast changes Δs_t^n are significant and negative in the high demand quota regime, but never significant in the low regime for all contracts. In hour H18, the coefficients of Δs_t^n are generally not significant. The negative sign of the coefficients is economically meaningful as electricity prices should increase if less solar power is forecasted. In Kiesel and Paraschiv (2017), the coefficients of Δs_t^n are also negative in the high regimes but only significant for some contracts. In the high demand quota regimes, the coefficients of Δs_t^n are at least three times larger by absolute value than in the low regimes.

The high regime implies that much renewable power infeed is expected; if solar forecast changes are negative, they contradict our expectation of the electricity generation mix established day-ahead and thus influence electricity prices more severely than in the low regime. In Kiesel and Paraschiv (2017), this asymmetry is less or not at all pronounced.

The coefficients of positive solar forecast changes Δs_t^p are significant and negative in both regimes for contracts H13Q1–Q3, while in hours H7 and H18, the coefficients of Δs_t^p are rarely significant and mostly negative. The negative sign is intuitive: If the expectation of solar power at time t is larger than at time $t-1$, $s_t > s_{t-1}$, the electricity price should decrease. In the low demand quota regimes in hour H13, the coefficients of Δs_t^p are two to four times larger than in the high regimes. The low regime implies that little renewable power production is anticipated; it is reasonable that positive solar forecast changes in the low regime decrease electricity prices more severely than in the high regime where more renewable power infeed is planned anyway. Our results confirm the findings of Kiesel and Paraschiv (2017).

Eventually, intraday price changes of 15-minute contracts are driven by both autoregressive terms and fundamental variables at noon. In morning and evening hours, however, intraday trading is primarily affected by autoregressive price changes.

4.2 Extended fundamental model

We estimate the coefficients of the extended fundamental model (2) by the threshold regression described in Section 3.3 for all 96 15-minute contracts. As representatives of morning, noon, and evening hours, we exemplarily analyze 15-minute contracts H7, H13, H18, Q1–Q4 each. For all contracts, the merit-order-curve slope ξ is used as threshold variable.

4.2.1 Estimation of merit-order-curve slope

We estimate the slope of the merit order curve $\xi^{(i)}$ of 15-minute contract i based on intraday auction prices $P^{\mathrm{Auc},(i)}$ and corresponding expected demands, or total load forecasts, $\ell^{(i)}$. As both $P^{\mathrm{Auc},(i)}$ and $\ell^{(i)}$ are provided in quarter-hourly resolution, we are able to determine a merit order curve for each 15-minute contract i individually. Figure 5 depicts a scatter plot of empirical intraday auction prices $P_d^{\mathrm{Auc},(i)}$ versus empirical expected demands $\ell_d^{(i)}$ observed on days $d = 1, \ldots, T$, for contract $i = \text{H13Q4}$. We filter out a total of 13 negative auction prices. We observe a positive relationship between intraday auction prices and expected demands: $P_d^{\mathrm{Auc},(i)}$ increases as $\ell_d^{(i)}$ increases. For high levels of demand, more expensive generation technologies are in use which puts upward pressure on prices. In particular, we may identify two clusters: One cluster encompasses expected demands $\ell < 58$ GW, and the other cluster comprises $\ell \geq 58$ GW. These clusters reflect low and high electricity demand on weekends and weekdays, respectively. Overall the data points exhibit a fairly wide range of variation which stems from the strongly varying expectation of renewable power infeed.

For the empirical merit order curve $f(\ell)$, we use the exponential function $f(\ell) = \mathrm{e}^{a\,\ell+b}$ following He et al. (2013). Of course other choices for $f(\ell)$ are possible, but we want to keep our model as simple as possible. We fit the exponential function $f(\ell)$ to the empirical intraday auction price $P^{\mathrm{Auc},(i)}$ as a function of expected demand $\ell^{(i)}$. Technically, we minimize the sum of squared errors between the logarithm of the function $f^{\Phi}(\ell)$ implied by the choice of a parameter set $\Phi = \{a, b\}$, and the logarithm of the empirical intraday auction price $P_d^{\mathrm{Auc},(i)}\left(\ell_d^{(i)}\right)$,

$$\min_{\Phi} \sum_{d=1}^{T} \left| \log\left(P_d^{\mathrm{Auc},(i)}\left(\ell_d^{(i)}\right)\right) - \log\left(f^{\Phi}(\ell)\right) \right|^2. \tag{11}$$

The least squares fit for contract $i = \text{H13Q4}$ is shown in Figure 5. The parameter estimates of a, b for contracts H7, H13, H18, Q1–Q4 each, are reported in Table 4.

H13Q1

Variable	Regime 1 $DQ \leq 1.100^{***}$ Estimate	Std error	Regime 2 $DQ > 1.100^{***}$ Estimate	Std error
Const	−1.337	(0.990)	−0.391	(1.725)
DQ	1.466	(0.977)	0.361	(1.464)
ΔP_{t-1}	−0.318***	(0.026)	−0.269***	(0.024)
ΔP_{t-2}	−0.151***	(0.021)	−0.072***	(0.018)
ΔP_{t-3}	−0.093***	(0.025)	−0.059**	(0.019)
V_t	−0.022***	(0.004)	−0.014***	(0.004)
Δw_t^n	−1.137***	(0.322)	−1.180***	(0.260)
Δw_t^p	−0.796*	(0.332)	−0.587	(0.303)
Δs_t^n	0.111	(0.428)	−1.730***	(0.534)
Δs_t^p	−3.545***	(0.492)	−1.374***	(0.428)
Δt	0.092***	(0.020)	0.061***	(0.021)
#Obs	6499		6554	
R_{adj}^2	0.159		0.144	

H13Q2

Variable	Regime 1 $DQ \leq 1.065^{***}$ Estimate	Std error	Regime 2 $DQ > 1.065^{***}$ Estimate	Std error
Const	−1.403	(1.534)	−1.765	(1.455)
DQ	1.600	(1.574)	1.441	(1.239)
ΔP_{t-1}	−0.281***	(0.028)	−0.304***	(0.029)
ΔP_{t-2}	−0.142***	(0.024)	−0.093***	(0.019)
ΔP_{t-3}	−0.047*	(0.025)	0.014	(0.030)
V_t	−0.022***	(0.007)	−0.005	(0.008)
Δw_t^n	−1.300***	(0.351)	−1.175***	(0.245)
Δw_t^p	−0.606	(0.378)	−0.220	(0.208)
Δs_t^n	−0.390	(0.552)	−1.738***	(0.385)
Δs_t^p	−3.442***	(0.432)	−1.329**	(0.438)
Δt	0.053	(0.026)	0.035	(0.019)
#Obs	4279		7764	
R_{adj}^2	0.123		0.137	

H13Q3

Variable	Regime 1 $DQ \leq 1.019^{*}$ Estimate	Std error	Regime 2 $DQ > 1.019^{*}$ Estimate	Std error
Const	0.574	(1.825)	−2.007	(1.175)
DQ	−0.877	(1.950)	1.507	(1.023)
ΔP_{t-1}	−0.270***	(0.028)	−0.269***	(0.021)
ΔP_{t-2}	−0.116***	(0.030)	−0.138	(0.019)
ΔP_{t-3}	−0.027	(0.023)	−0.073	(0.016)
V_t	0.014*	(0.008)	0.012	(0.004)
Δw_t^n	−0.892*	(0.479)	−1.125	(0.254)
Δw_t^p	−0.134	(0.318)	−0.522	(0.219)
Δs_t^n	0.204	(0.449)	−2.063***	(0.446)
Δs_t^p	−2.292***	(0.518)	−1.267	(0.461)
Δt	−0.023	(0.028)	0.026	(0.019)
#Obs	3538		9278	
R_{adj}^2	0.087		0.125	

H13Q4

Variable	Regime 1 $DQ \leq 1.148^{***}$ Estimate	Std error	Regime 2 $DQ > 1.148^{***}$ Estimate	Std error
Const	−2.969	(0.712)	−4.635	(2.765)
DQ	2.609	(0.671)	3.765	(2.299)
ΔP_{t-1}	−0.292***	(0.021)	−0.219***	(0.023)
ΔP_{t-2}	−0.128***	(0.015)	−0.102***	(0.021)
ΔP_{t-3}	−0.049***	(0.014)	−0.094***	(0.020)
V_t	0.014**	(0.003)	0.007	(0.003)
Δw_t^n	−1.527***	(0.298)	−1.203***	(0.313)
Δw_t^p	−0.355	(0.220)	−0.299	(0.443)
Δs_t^n	−0.811	(0.333)	−3.001***	(0.684)
Δs_t^p	−0.450	(0.498)	−1.779	(0.696)
Δt	−0.036	(0.020)	−0.025	(0.027)
#Obs	10 372		4782	
R_{adj}^2	0.110		0.149	

$^{*}p < 0.1;\ ^{**}p < 0.05;\ ^{***}p < 0.01$

Table 1: Estimation results of the benchmark fundamental model (1) for 15-minute contracts H13Q1–4.

H7Q1

Variable	Regime 1 $DQ \leq 1.022^{***}$ Estimate	Std error	Regime 2 $DQ > 1.022^{***}$ Estimate	Std error
Const	1.277	(1.613)	−0.575	(2.142)
DQ	−2.147	(1.833)	−0.379	(1.896)
ΔP_{t-1}	−0.332***	(0.031)	−0.375***	(0.025)
ΔP_{t-2}	−0.148***	(0.031)	−0.169***	(0.021)
ΔP_{t-3}	−0.087***	(0.028)	−0.063***	(0.018)
V_t	0.043***	(0.006)	0.038***	(0.003)
Δw_t^n	−1.271	(0.742)	−0.808**	(0.353)
Δw_t^p	−1.331***	(0.383)	−0.577**	(0.265)
Δs_t^n	8.318	(4.777)	−3.889	(4.843)
Δs_t^p	−6.672	(5.434)	8.814*	(4.036)
Δt	−0.094	(0.050)	0.093**	(0.034)
#Obs	3092		6953	
R^2_{adj}	0.157		0.160	

H7Q2

Variable	Regime 1 $DQ \leq 1.042^{***}$ Estimate	Std error	Regime 2 $DQ > 1.042^{***}$ Estimate	Std error
Const	0.332	(1.557)	0.668	(2.484)
DQ	−0.748	(1.743)	−1.099	(2.180)
ΔP_{t-1}	−0.307***	(0.026)	−0.303***	(0.023)
ΔP_{t-2}	−0.180***	(0.025)	−0.128***	(0.018)
ΔP_{t-3}	−0.100***	(0.021)	−0.083***	(0.016)
V_t	0.059***	(0.012)	0.021**	(0.008)
Δw_t^n	−0.376	(0.600)	−0.686**	(0.264)
Δw_t^p	−1.471***	(0.430)	−0.622*	(0.322)
Δs_t^n	2.863	(2.657)	−8.558*	(4.051)
Δs_t^p	−2.338	(4.187)	1.673	(2.340)
Δt	−0.145**	(0.046)	0.113***	(0.033)
#Obs	2813		6180	
R^2_{adj}	0.161		0.111	

H7Q3

Variable	Regime 1 $DQ \leq 1.053^{***}$ Estimate	Std error	Regime 2 $DQ > 1.053^{***}$ Estimate	Std error
Const	−1.927	(1.514)	−2.104	(2.772)
DQ	2.532	(1.646)	1.670	(2.429)
ΔP_{t-1}	−0.322***	(0.026)	−0.321***	(0.029)
ΔP_{t-2}	−0.139***	(0.024)	−0.148***	(0.022)
ΔP_{t-3}	−0.061**	(0.022)	−0.093***	(0.021)
V_t	−0.026**	(0.010)	−0.020***	(0.006)
Δw_t^n	−0.111	(0.568)	−0.781*	(0.356)
Δw_t^p	−0.636	(0.335)	−0.281	(0.402)
Δs_t^n	2.767	(2.280)	−10.365*	(4.773)
Δs_t^p	−3.519	(3.005)	−1.861	(1.975)
Δt	−0.085	(0.043)	0.131***	(0.035)
#Obs	3154		6399	
R^2_{adj}	0.113		0.139	

H7Q4

Variable	Regime 1 $DQ \leq 1.156^{***}$ Estimate	Std error	Regime 2 $DQ > 1.156^{***}$ Estimate	Std error
Const	−2.178	(0.781)	−1.898	(5.697)
DQ	2.115	(0.743)	1.422	(4.773)
ΔP_{t-1}	−0.332***	(0.019)	−0.228***	(0.034)
ΔP_{t-2}	−0.154***	(0.016)	−0.101***	(0.029)
ΔP_{t-3}	−0.061	(0.015)	−0.039	(0.033)
V_t	−0.014*	(0.003)	−0.014**	(0.005)
Δw_t^n	−0.888	(0.400)	−0.187	(0.647)
Δw_t^p	−1.075**	(0.307)	0.716	(0.472)
Δs_t^n	1.202	(2.256)	−8.426**	(3.314)
Δs_t^p	−6.350**	(2.088)	−3.800	(2.609)
Δt	0.064	(0.033)	0.164**	(0.053)
#Obs	8308		3173	
R^2_{adj}	0.126		0.122	

$^{*}p < 0.1$; $^{**}p < 0.05$; $^{***}p < 0.01$

Table 2: Estimation results of the benchmark fundamental model (1) for 15-minute contracts H7Q1–4.

H18Q1

| | Regime 1 | | Regime 2 | |
| | $DQ \leq 1.135$ | | $DQ > 1.135$ | |
Variable	Estimate	Std error	Estimate	Std error
Const	0.151	(0.984)	9.257	(7.735)
DQ	0.075	(0.916)	−7.531	(6.525)
ΔP_{t-1}	−0.278**	(0.039)	−0.431**	(0.174)
ΔP_{t-2}	−0.115	(0.022)	−0.176	(0.166)
ΔP_{t-3}	−0.018	(0.020)	0.077	(0.128)
V_t	−0.003	(0.003)	−0.012	(0.005)
Δw_t^n	−1.831	(0.243)	−0.609	(0.729)
Δw_t^p	−0.539	(0.606)	−2.141	(0.546)
Δs_t^n	−1.823	(1.332)	−2.994	(3.769)
Δs_t^p	−4.223	(1.224)	−2.563	(2.356)
Δt	−0.052	(0.015)	−0.036	(0.042)
#Obs	9790		2403	
R^2_{adj}	0.105		0.194	

H18Q2

| | Regime 1 | | Regime 2 | |
| | $DQ \leq 1.118^*$ | | $DQ > 1.118^*$ | |
Variable	Estimate	Std error	Estimate	Std error
Const	−0.145	(1.045)	−1.549	(5.186)
DQ	0.180	(0.986)	1.364	(4.503)
ΔP_{t-1}	−0.322***	(0.019)	−0.277***	(0.029)
ΔP_{t-2}	−0.112**	(0.016)	−0.138***	(0.023)
ΔP_{t-3}	−0.063	(0.014)	−0.010	(0.020)
V_t	0.010	(0.006)	−0.006	(0.007)
Δw_t^n	0.101	(0.618)	−3.040	(1.238)
Δw_t^p	−1.736**	(0.371)	0.652	(0.668)
Δs_t^n	−0.848	(1.465)	1.752	(3.483)
Δs_t^p	−1.716	(1.551)	0.654	(1.895)
Δt	−0.016	(0.016)	−0.015	(0.029)
#Obs	7672		2973	
R^2_{adj}	0.121		0.105	

H18Q3

| | Regime 1 | | Regime 2 | |
| | $DQ \leq 1.144$ | | $DQ > 1.144$ | |
Variable	Estimate	Std error	Estimate	Std error
Const	−0.443	(0.893)	5.784	(9.044)
DQ	0.236	(0.838)	−4.823	(7.749)
ΔP_{t-1}	−0.308***	(0.016)	−0.291***	(0.044)
ΔP_{t-2}	−0.150***	(0.016)	−0.045	(0.032)
ΔP_{t-3}	−0.044***	(0.012)	−0.009	(0.026)
V_t	0.006	(0.007)	−0.008	(0.011)
Δw_t^n	−0.423	(0.326)	−3.505***	(0.822)
Δw_t^p	−1.480**	(0.673)	2.335	(2.162)
Δs_t^n	−4.480**	(1.830)	0.073	(2.401)
Δs_t^p	−0.267	(1.432)	16.354**	(7.125)
Δt	0.018	(0.014)	−0.066	(0.055)
#Obs	9745		1249	
R^2_{adj}	0.112		0.155	

H18Q4

| | Regime 1 | | Regime 2 | |
| | $DQ \leq 1.171$ | | $DQ > 1.171$ | |
Variable	Estimate	Std error	Estimate	Std error
Const	−0.378	(0.730)	21.412	(39.252)
DQ	0.279	(0.693)	−17.492	(32.591)
ΔP_{t-1}	−0.312***	(0.021)	−0.386*	(0.212)
ΔP_{t-2}	−0.126***	(0.016)	−0.118	(0.148)
ΔP_{t-3}	−0.030	(0.013)	−0.266	(0.101)
V_t	0.001	(0.002)	0.051	(0.027)
Δw_t^n	−1.897	(0.977)	2.568	(5.729)
Δw_t^p	−0.180	(0.297)	−5.008	(3.700)
Δs_t^n	1.935	(1.927)	7.501	(6.666)
Δs_t^p	−4.024*	(1.563)	4.548	(6.819)
Δt	0.008	(0.016)	−0.130	(0.127)
#Obs	12 779		326	
R^2_{adj}	0.115		0.231	

$^*p < 0.1$; $^{**}p < 0.05$; $^{***}p < 0.01$

Table 3: Estimation results of the benchmark fundamental model (1) for 15-minute contracts H18Q1–4.

We observe an hourly seasonality of the parameter estimates $\hat{a}, \hat{b}$. For contracts H4Q1–H14Q4, the estimates $\hat{a}, \hat{b}$ increase and decrease from the first to the last 15-minute contract within an hour, respectively, whereas for contracts H15Q1–H2Q4, the estimates $\hat{a}, \hat{b}$ decrease and increase, respectively. Thus the curvature of the empirical merit order curve $f(\ell)$ grows from Q1 to Q4 in each hour during morning and noon hours, whereas it declines from Q1 to Q4 during afternoon and evening hours. This hourly seasonality may be associated with rising and falling demand in the first and second half of the day, respectively, following human activity (Paraschiv, 2013). Consequently, in the first half of the day, more expensive power plants are needed to cover demand in the last than in the first quarter-hour in each hour, whereas in the second half of the day, more expensive power plants are operated in the first than in the last quarter-hour per hour.

Eventually, we take the derivative of the fitted merit-order-curve function $f'^{\,\Phi}(\ell) = \frac{\mathrm{d}f^{\Phi}(\ell)}{\mathrm{d}\ell}$ and substitute empirical expected loads $\ell_d^{(i)}$ into $f'^{\,\Phi}(\ell)$ to obtain empirical merit-order-curve slopes $\xi_d^{(i)} = f'^{\,\Phi}\left(\ell_d^{(i)}\right)$ on days $d = 1, \dots, T$, for 15-minute contract i.
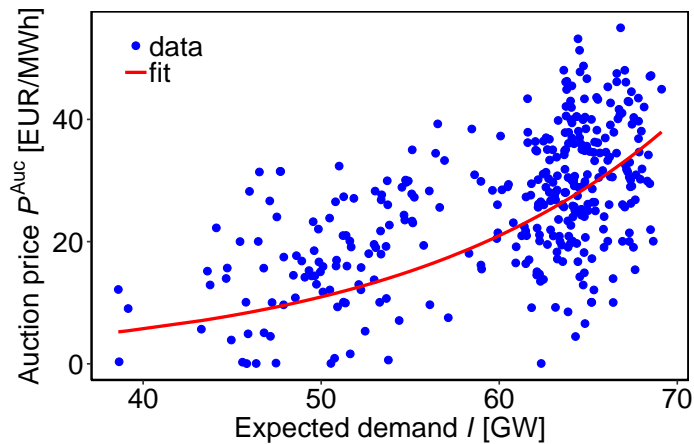
Figure 5: Empirical merit-order-curve function $f(\ell) = \mathrm{e}^{a\,\ell+b}$ (red) fitted to the empirical intra-day auction price $P_d^{\mathrm{Auc},(i)}$ as a function of expected demand $\ell_d^{(i)}$ (blue) observed on days $d = 1, \dots, T$, for 15-minute contract $i = $ H13Q4.

4.2.2 Model calibration

The estimation results of all 15-minute contracts in hours H13, H7, H18 are presented in Tables 5, 6, 7, respectively. The threshold parameter estimate is highly statistically significant in hours H13 and H7, while in hour H18, it is only statistically significant for contract Q2. A merit-order-curve slope of $\xi = 1\,\frac{\mathrm{EUR/MWh}}{\mathrm{GW}}$ implies that a change of 1 GW in expected demand causes a change of 1 EUR/MWh in the intraday auction price. Regime 1 corresponds to a market in which the merit order curve is flat, whereas Regime 2 reflects a market in which the merit order curve is steep. For all contracts, the total sample is split into subsamples of appropriate size and enables us to interpret the estimation results adequately.

The adjusted R^2 ranges between 11% and 30%. Thus, overall, our extended fundamental model exhibits higher explanatory power in explaining intraday price changes ΔP_t than the benchmark model by Kiesel and Paraschiv (2017). In particular, our extended fundamental model outnumbers the benchmark model's adjusted R^2 for each contract and regime in hours H13 and H7. In hour H18, the extended model only marginally improves the explanation of intraday price changes ΔP_t for contracts Q1 and Q2 compared to the benchmark model.

The estimated coefficients of the autoregressive terms $\Delta P_{t-1}, \Delta P_{t-2}$ are highly statistically significant and negative in both regimes for all contracts, and even the coefficients of ΔP_{t-3} are significant and negative in most cases. For evening contracts, the higher-order autoregressive

	Parameter			
	a		b	
Contract	Estimate	Std error	Estimate	Std error
H7Q1	0.029	(0.004)	1.632	(0.268)
H7Q2	0.036	(0.002)	1.412	(0.134)
H7Q3	0.045	(0.002)	0.961	(0.125)
H7Q4	0.045	(0.002)	0.940	(0.130)
H13Q1	0.022	(0.002)	2.194	(0.141)
H13Q2	0.037	(0.003)	1.214	(0.201)
H13Q3	0.045	(0.004)	0.548	(0.217)
H13Q4	0.065	(0.006)	-0.856	(0.389)
H18Q1	0.061	(0.005)	-0.372	(0.313)
H18Q2	0.039	(0.003)	1.246	(0.160)
H18Q3	0.021	(0.002)	2.546	(0.109)
H18Q4	0.013	(0.002)	3.074	(0.140)

Table 4: Parameter estimates of a, b of the empirical merit-order-curve function $f(\ell) = e^{a\,\ell+b}$ for 15-minute contracts H7, H13, H18, Q1–Q4 each.

terms show less statistical significance. The negative coefficients of lagged price changes suggest mean reversion in the price formation process of 15-minute contracts. We recall that Kiesel and Paraschiv (2017) find less significance of autoregressive terms during noon hours when renewable forecast changes primarily dominate the intraday trading. We, however, provide evidence of a significant mean reversion effect for noon contracts in 2015.

In hour H13, the estimated coefficients of price changes of neighboring contracts $\Delta P_t^{(i-2)}$, $\Delta P_t^{(i-1)}$, $\Delta P_t^{(i+1)}$ are highly statistically significant and positive in both regimes for all contracts, while the coefficients of $\Delta P_t^{(i+2)}$ are significant and positive in the steep merit-order regime only. In hour H7, the estimated coefficients of price changes of neighboring contracts $\Delta P_t^{(i-2)}, \ldots, \Delta P_t^{(i+2)}$ are highly statistically significant and positive in the steep merit-order regime for all contracts, while the coefficients of $\Delta P_t^{(i-1)}, \Delta P_t^{(i+1)}$ are significant and positive in the flat regime for contracts Q2 and Q3, too. Thus price changes of neighboring contracts have strong explanatory power and a positive effect on one another. In particular, we observe that price changes of the nearest neighbors $i\pm1$ have a stronger impact on price changes of contract i than price changes of next-nearest neighbors $i\pm2$ [4]. For contracts Q1, price changes $\Delta P_t^{(i+1)}$ of the following contracts Q2 have the greatest influence, whereas for contracts Q4, price changes $\Delta P_t^{(i-1)}$ of the preceding contracts Q3 exhibit the largest impact. Hence 15-minute contracts within the same hour are the most important price drivers. In hour H18, the coefficients of $\Delta P_t^{(i-2)}, \ldots, \Delta P_t^{(i+2)}$ are rarely statistically significant.

The coefficients of the intraday auction price P^{Auc} are not significant for all contracts and regimes. This is not surprising since P^{Auc} can merely be considered as an estimate of the initial price of a 15-minute contract in the continuous trading. Thus it is not expected that P^{Auc} affects continuous trading beyond the first price.

In hour H13, the coefficients of trading volume V_t are only significant in the steep merit-order regime for contracts Q1, Q3, Q4. Independent of the regime, they are negative for Q1 and Q2 and positive for Q3 and Q4. This sign profile illustrates the joint hourly seasonality of

---

[4] The terms nearest and next-nearest neighbors are motivated from physics where a nearest- and next-nearest-neighbor interaction exists.

intraday prices and volumes presented in Section 2.2: As more solar power is generated than the hourly average in Q1 and Q2, there is sell pressure at the beginning of the hour and intraday prices decrease. Conversely, buy pressure increases intraday prices at the end of the hour when below-average solar power is produced. In hour H7, the coefficients of V_t are significant for all contracts and regimes. For contracts Q1 and Q2 they are positive, whereas for Q3 and Q4 they turn negative independent of the regime. Thereby the positive and negative coefficients reflect buy and sell pressure in line with the hourly seasonality. In hour H18, the coefficients of V_t are not significant. In general, we do not find an asymmetric adjustment of intraday price changes ΔP_t to trading volumes V_t.

Overall the coefficients of negative wind forecast changes Δw_t^n are significant and negative in the steep merit-order regime for all contracts. The negative sign is reasonable as electricity prices should increase if less wind power is forecasted. In hour H13, the coefficients of positive wind forecast changes Δw_t^p are only significant and negative in the steep regime for Q1 and Q3. In hour H7, the coefficients of Δw_t^p are significant and negative in both regimes for Q1 and Q2, while in hour H18, they are significant and negative in both regimes for Q3. No asymmetry in the coefficients of wind forecast changes between the regimes is observed.

The coefficients of negative solar forecast changes Δs_t^n are significant and negative in the steep merit-order regime, but not significant in the flat regime for contracts in hours H13 and H7. In hour H18, the coefficients of Δs_t^n are significant in both regimes for Q3. In the steep regimes, the coefficients of Δs_t^n are at least two times larger by absolute value than in the flat regimes. This reflects the fact that renewable forecast changes affect electricity prices more severely in the steep than in the flat merit-order regime. In hour H13, the coefficients of positive solar forecast changes Δs_t^p are significant and negative in both regimes for contracts Q1–Q3. In hour H7, the coefficients of Δs_t^p are significant and negative in both regimes for Q4, while in hour H18, they are generally not significant. The negative sign is intuitive as a larger expectation of solar power should decrease electricity prices.

Generally, renewable forecast changes are more significant in the steep than in the flat merit-order regime. When the market is in the steep merit-order regime, market participants rely on the use of more expensive power generation technologies, which sets additional pressure on them to balance the volatile renewable energies on the intraday market.

Eventually, intraday trading of 15-minute contracts is driven by both trade and fundamental data at noon, while trade data have a slight surplus importance. For morning and evening contracts, however, intraday price changes are predominantly influenced by trade data.

5 Conclusion

This paper develops a fundamental price model for continuous intraday electricity markets of 15-minute contracts. We analyze a novel and unique data set of high-frequency transaction data, fundamental supply and demand data, and intradaily updated forecasts of wind and solar power generation. The nature of our data set allows the model specification to solely include *ex-ante* market information.

We perform an empirical exploration of transaction prices and trading volumes of 15-minute contracts. Empirical evidence suggests that, on average, transaction prices of 15-minute contracts exhibit a sawtooth-shaped and trading volumes a U-shaped hourly seasonality. Moreover, liquidity increases sharply within the last trading hour before gate closure. Our empirical analysis also indicates that renewable forecast updates are reflected in intraday prices within one trading minute.

We refine the fundamental model by Kiesel and Paraschiv (2017) along three main dimensions by incorporating: (i) the slope of the merit order curve, (ii) price changes of neighboring 15-minute contracts, (iii) the 15-minute intraday auction price. We calibrate our fundamental model to market data for a selection of morning, noon, and evening contracts. A threshold

H13Q1

Variable	Regime 1 $\xi \leq 0.689^{**}$		Regime 2 $\xi > 0.689^{**}$	
	Estimate	Std error	Estimate	Std error
Const	-2.197	(1.598)	-0.615	(0.886)
ξ	3.599	(2.597)	0.685	(1.025)
ΔP_{t-1}	-0.388^{***}	(0.040)	-0.339^{***}	(0.018)
ΔP_{t-2}	-0.200^{***}	(0.029)	-0.153^{***}	(0.015)
ΔP_{t-3}	-0.136^{***}	(0.034)	-0.090^{***}	(0.014)
$\Delta P_t^{(i-2)}$	0.054^{**}	(0.025)	0.029^{**}	(0.010)
$\Delta P_t^{(i-1)}$	0.092^{***}	(0.023)	0.067^{***}	(0.013)
$\Delta P_t^{(i+1)}$	0.188^{***}	(0.035)	0.191^{***}	(0.015)
$\Delta P_t^{(i+2)}$	0.076^{**}	(0.029)	0.040^{**}	(0.010)
P^{Auc}	0.004	(0.014)	0.002	(0.006)
V_t	-0.026	(0.006)	-0.015^{***}	(0.003)
Δw_t^n	-0.523	(0.376)	-1.086^{***}	(0.201)
Δw_t^p	-0.634	(0.371)	-0.635^{**}	(0.243)
Δs_t^n	0.729	(0.327)	-1.531^{**}	(0.412)
Δs_t^p	-2.661^{**}	(0.449)	-1.784^{***}	(0.386)
Δt	0.096	(0.029)	0.059^{***}	(0.016)
#Obs	3131		9922	
R^2_{adj}	0.236		0.227	

H13Q2

Variable	Regime 1 $\xi \leq 1.115^{***}$		Regime 2 $\xi > 1.115^{***}$	
	Estimate	Std error	Estimate	Std error
Const	-0.449	(0.741)	-0.171	(0.921)
ξ	1.352	(0.861)	-0.109	(0.677)
ΔP_{t-1}	-0.338^{***}	(0.029)	-0.360^{***}	(0.024)
ΔP_{t-2}	-0.181^{***}	(0.024)	-0.147^{***}	(0.017)
ΔP_{t-3}	-0.065^{*}	(0.023)	-0.032	(0.021)
$\Delta P_t^{(i-2)}$	0.093^{***}	(0.023)	0.076^{***}	(0.014)
$\Delta P_t^{(i-1)}$	0.277^{***}	(0.030)	0.267^{***}	(0.022)
$\Delta P_t^{(i+1)}$	0.150^{***}	(0.024)	0.177^{***}	(0.024)
$\Delta P_t^{(i+2)}$	0.046	(0.027)	0.055^{***}	(0.017)
P^{Auc}	-0.015	(0.017)	0.008	(0.007)
V_t	-0.021^{**}	(0.007)	-0.003	(0.007)
Δw_t^n	-0.828	(0.329)	-0.960^{***}	(0.188)
Δw_t^p	-0.527	(0.255)	-0.069	(0.170)
Δs_t^n	-0.166	(0.444)	-1.439^{***}	(0.289)
Δs_t^p	-2.230^{***}	(0.314)	-1.064^{***}	(0.357)
Δt	0.019	(0.025)	0.024	(0.016)
#Obs	3742		8301	
R^2_{adj}	0.238		0.267	

H13Q3

Variable	Regime 1 $\xi \leq 1.293^{***}$		Regime 2 $\xi > 1.293^{***}$	
	Estimate	Std error	Estimate	Std error
Const	-0.309	(0.414)	-0.172	(0.816)
ξ	0.666	(0.598)	0.126	(0.546)
ΔP_{t-1}	-0.309^{***}	(0.026)	-0.321^{***}	(0.021)
ΔP_{t-2}	-0.153^{**}	(0.025)	-0.166^{***}	(0.019)
ΔP_{t-3}	-0.059	(0.019)	-0.083^{***}	(0.015)
$\Delta P_t^{(i-2)}$	0.069	(0.021)	0.055^{***}	(0.015)
$\Delta P_t^{(i-1)}$	0.121^{***}	(0.020)	0.199^{***}	(0.026)
$\Delta P_t^{(i+1)}$	0.195^{***}	(0.026)	0.320^{***}	(0.026)
$\Delta P_t^{(i+2)}$	0.063	(0.021)	0.043^{***}	(0.012)
P^{Auc}	-0.019	(0.019)	-0.007	(0.007)
V_t	0.011	(0.006)	0.011^{**}	(0.004)
Δw_t^n	-0.683	(0.303)	-0.564^{***}	(0.175)
Δw_t^p	-0.138	(0.202)	-0.445^{*}	(0.204)
Δs_t^n	0.093	(0.392)	-1.737^{***}	(0.394)
Δs_t^p	-1.640^{***}	(0.303)	-0.816^{*}	(0.403)
Δt	-0.017	(0.022)	0.028	(0.019)
#Obs	4940		7876	
R^2_{adj}	0.174		0.296	

H13Q4

Variable	Regime 1 $\xi \leq 1.605$		Regime 2 $\xi > 1.605$	
	Estimate	Std error	Estimate	Std error
Const	-0.982	(0.287)	-0.780	(0.514)
ξ	0.638	(0.267)	0.097	(0.269)
ΔP_{t-1}	-0.318^{***}	(0.023)	-0.323^{***}	(0.019)
ΔP_{t-2}	-0.160^{***}	(0.019)	-0.162^{***}	(0.015)
ΔP_{t-3}	-0.090^{***}	(0.016)	-0.085^{***}	(0.017)
$\Delta P_t^{(i-2)}$	0.054^{***}	(0.015)	0.078^{***}	(0.015)
$\Delta P_t^{(i-1)}$	0.192^{***}	(0.021)	0.213^{***}	(0.017)
$\Delta P_t^{(i+1)}$	0.116^{***}	(0.042)	0.053^{***}	(0.013)
$\Delta P_t^{(i+2)}$	0.023	(0.016)	0.051^{**}	(0.014)
P^{Auc}	0.004	(0.011)	0.010	(0.006)
V_t	0.012	(0.004)	0.012^{***}	(0.003)
Δw_t^n	-1.469^{**}	(0.398)	-1.017^{***}	(0.232)
Δw_t^p	-0.259	(0.252)	-0.543	(0.246)
Δs_t^n	-0.472	(0.360)	-2.503^{***}	(0.433)
Δs_t^p	-1.056	(0.453)	0.254	(0.497)
Δt	-0.041	(0.024)	-0.037	(0.020)
#Obs	6367		8787	
R^2_{adj}	0.172		0.237	

$^{*}p < 0.1;\ ^{**}p < 0.05;\ ^{***}p < 0.01$

Table 5: Estimation results of the extended fundamental model (2) for 15-minute contracts H13Q1–4.

H7Q1

Variable	Regime 1 $\xi \leq 0.700^{***}$ Estimate	Std error	Regime 2 $\xi > 0.700^{***}$ Estimate	Std error
Const	2.642^{*}	(1.210)	-0.384	(1.190)
ξ	-6.105^{***}	(2.013)	-0.383	(1.142)
ΔP_{t-1}	-0.360^{***}	(0.033)	-0.397^{***}	(0.023)
ΔP_{t-2}	-0.189^{***}	(0.033)	-0.187^{***}	(0.020)
ΔP_{t-3}	-0.121^{***}	(0.030)	-0.066^{***}	(0.018)
$\Delta P_t^{(i-2)}$	0.020	(0.021)	0.026^{**}	(0.013)
$\Delta P_t^{(i-1)}$	0.020	(0.024)	0.030^{**}	(0.014)
$\Delta P_t^{(i+1)}$	0.171^{***}	(0.029)	0.102^{***}	(0.016)
$\Delta P_t^{(i+2)}$	0.019	(0.024)	0.078^{***}	(0.015)
P^{Auc}	0.014	(0.016)	-0.008	(0.010)
V_t	0.041^{***}	(0.006)	0.038^{***}	(0.003)
Δw_t^n	0.094	(0.817)	-1.216^{***}	(0.268)
Δw_t^p	-1.313^{***}	(0.357)	-0.649^{***}	(0.244)
Δs_t^n	7.095	(4.622)	-5.600	(3.885)
Δs_t^p	0.149	(5.442)	6.780^{*}	(4.040)
Δt	-0.087^{*}	(0.048)	0.081^{**}	(0.032)
#Obs	2898		7147	
R^2_{adj}	0.198		0.193	

H7Q2

Variable	Regime 1 $\xi \leq 1.111^{***}$ Estimate	Std error	Regime 2 $\xi > 1.111^{***}$ Estimate	Std error
Const	0.366	(0.939)	-0.334	(0.981)
ξ	-0.650	(1.156)	-0.112	(0.605)
ΔP_{t-1}	-0.349^{***}	(0.025)	-0.329^{***}	(0.021)
ΔP_{t-2}	-0.206^{***}	(0.025)	-0.154^{***}	(0.017)
ΔP_{t-3}	-0.117^{***}	(0.021)	-0.094^{***}	(0.015)
$\Delta P_t^{(i-2)}$	0.035	(0.020)	0.014	(0.014)
$\Delta P_t^{(i-1)}$	0.263^{***}	(0.029)	0.140^{***}	(0.017)
$\Delta P_t^{(i+1)}$	0.097^{***}	(0.025)	0.117^{***}	(0.019)
$\Delta P_t^{(i+2)}$	0.077^{***}	(0.024)	0.082^{***}	(0.016)
P^{Auc}	-0.006	(0.017)	-0.002	(0.013)
V_t	0.060^{***}	(0.012)	0.020^{**}	(0.008)
Δw_t^n	0.144	(0.438)	-0.765^{***}	(0.208)
Δw_t^p	-1.342^{***}	(0.403)	-0.605^{**}	(0.290)
Δs_t^n	0.629	(2.280)	-9.681^{***}	(3.467)
Δs_t^p	-0.281	(3.216)	0.788	(2.152)
Δt	-0.138^{***}	(0.040)	0.100^{***}	(0.029)
#Obs	2647		6346	
R^2_{adj}	0.265		0.169	

H7Q3

Variable	Regime 1 $\xi \leq 1.403^{***}$ Estimate	Std error	Regime 2 $\xi > 1.403^{***}$ Estimate	Std error
Const	0.448	(0.747)	0.211	(0.734)
ξ	0.210	(0.856)	-0.170	(0.357)
ΔP_{t-1}	-0.387^{***}	(0.025)	-0.362^{***}	(0.028)
ΔP_{t-2}	-0.192^{***}	(0.024)	-0.180^{***}	(0.021)
ΔP_{t-3}	-0.087^{***}	(0.022)	-0.113^{***}	(0.019)
$\Delta P_t^{(i-2)}$	0.042	(0.022)	0.056^{***}	(0.014)
$\Delta P_t^{(i-1)}$	0.110^{***}	(0.022)	0.120^{***}	(0.015)
$\Delta P_t^{(i+1)}$	0.260^{***}	(0.027)	0.189^{***}	(0.021)
$\Delta P_t^{(i+2)}$	0.023	(0.025)	0.079^{**}	(0.031)
P^{Auc}	0.001	(0.018)	-0.002	(0.012)
V_t	-0.032^{***}	(0.010)	-0.020^{***}	(0.006)
Δw_t^n	0.222	(0.424)	-0.632	(0.338)
Δw_t^p	-0.634	(0.311)	-0.224	(0.341)
Δs_t^n	2.109	(1.908)	-10.170^{**}	(4.036)
Δs_t^p	-1.478	(2.598)	-2.136	(1.557)
Δt	-0.131^{***}	(0.038)	0.120^{***}	(0.029)
#Obs	2694		6859	
R^2_{adj}	0.223		0.215	

H7Q4

Variable	Regime 1 $\xi \leq 1.267^{***}$ Estimate	Std error	Regime 2 $\xi > 1.267^{***}$ Estimate	Std error
Const	-0.613	(0.853)	0.010	(0.511)
ξ	0.942	(0.948)	-0.236	(0.264)
ΔP_{t-1}	-0.373^{***}	(0.036)	-0.342^{***}	(0.018)
ΔP_{t-2}	-0.198^{***}	(0.033)	-0.162^{***}	(0.016)
ΔP_{t-3}	-0.078^{***}	(0.027)	-0.068^{***}	(0.017)
$\Delta P_t^{(i-2)}$	0.067^{***}	(0.025)	0.084^{***}	(0.011)
$\Delta P_t^{(i-1)}$	0.206^{***}	(0.027)	0.186^{***}	(0.018)
$\Delta P_t^{(i+1)}$	0.012	(0.031)	0.071^{***}	(0.016)
$\Delta P_t^{(i+2)}$	0.034	(0.032)	0.058^{***}	(0.013)
P^{Auc}	0.003	(0.015)	0.006	(0.009)
V_t	-0.012^{*}	(0.006)	-0.013^{***}	(0.003)
Δw_t^n	0.936	(0.772)	-0.752^{**}	(0.348)
Δw_t^p	-0.831^{**}	(0.370)	-0.410	(0.325)
Δs_t^n	2.750	(1.894)	-8.485^{***}	(2.359)
Δs_t^p	-6.181^{**}	(2.845)	-3.434^{**}	(1.600)
Δt	-0.073	(0.047)	0.128^{***}	(0.028)
#Obs	2750		8731	
R^2_{adj}	0.219		0.197	

$^{*}p < 0.1$; $^{**}p < 0.05$; $^{***}p < 0.01$

Table 6: Estimation results of the extended fundamental model (2) for 15-minute contracts H7Q1–4.

H18Q1

Variable	Regime 1 $\xi \leq 2.546$		Regime 2 $\xi > 2.546$	
	Estimate	Std error	Estimate	Std error
Const	0.151	(0.252)	4.748	(3.304)
ξ	0.057	(0.140)	-1.681	(1.240)
ΔP_{t-1}	-0.289^{***}	(0.036)	-0.433^{**}	(0.192)
ΔP_{t-2}	-0.118^{***}	(0.021)	-0.195	(0.181)
ΔP_{t-3}	-0.013	(0.019)	0.053	(0.138)
$\Delta P_t^{(i-2)}$	-0.003	(0.009)	0.018	(0.031)
$\Delta P_t^{(i-1)}$	-0.001	(0.007)	-0.004	(0.019)
$\Delta P_t^{(i+1)}$	0.033^{***}	(0.008)	-0.034	(0.037)
$\Delta P_t^{(i+2)}$	0.009	(0.009)	-0.041	(0.030)
P^{Auc}	0.003	(0.005)	0.005	(0.017)
V_t	-0.005^{*}	(0.003)	0.000	(0.006)
Δw_t^n	-1.739^{**}	(0.367)	-0.839	(0.958)
Δw_t^p	-0.619	(0.586)	-1.898^{**}	(0.873)
Δs_t^n	-2.231	(1.312)	2.510	(2.471)
Δs_t^p	-4.121^{***}	(1.092)	1.312	(1.800)
Δt	-0.054^{***}	(0.016)	-0.040	(0.039)
#Obs	10 142		2051	
R_{adj}^2	0.114		0.190	

H18Q2

Variable	Regime 1 $\xi \leq 1.906^{*}$		Regime 2 $\xi > 1.906^{*}$	
	Estimate	Std error	Estimate	Std error
Const	-0.002	(0.325)	-0.849	(12.290)
ξ	0.120	(0.250)	0.335	(6.205)
ΔP_{t-1}	-0.323^{***}	(0.016)	-0.166^{***}	(0.051)
ΔP_{t-2}	-0.127^{***}	(0.014)	-0.022	(0.043)
ΔP_{t-3}	-0.055^{***}	(0.012)	0.024	(0.041)
$\Delta P_t^{(i-2)}$	0.001	(0.006)	-0.024	(0.022)
$\Delta P_t^{(i-1)}$	0.026^{***}	(0.008)	0.038	(0.034)
$\Delta P_t^{(i+1)}$	0.013	(0.010)	-0.059^{*}	(0.028)
$\Delta P_t^{(i+2)}$	0.004	(0.009)	0.028	(0.024)
P^{Auc}	-0.004	(0.007)	0.007	(0.028)
V_t	0.006	(0.005)	-0.004	(0.021)
Δw_t^n	-0.128	(0.487)	-4.932^{***}	(0.561)
Δw_t^p	-1.336^{***}	(0.504)	1.578	(1.746)
Δs_t^n	-1.679	(1.292)	7.481^{***}	(1.150)
Δs_t^p	-1.038	(1.264)	0.245	(1.746)
Δt	-0.011	(0.014)	-0.099^{**}	(0.040)
#Obs	10 072		573	
R_{adj}^2	0.119		0.172	

H18Q3

Variable	Regime 1 $\xi \leq 1.015$		Regime 2 $\xi > 1.015$	
	Estimate	Std error	Estimate	Std error
Const	-1.187	(0.645)	-2.340	(9.064)
ξ	0.962	(0.822)	2.419	(8.660)
ΔP_{t-1}	-0.311^{***}	(0.017)	-0.306^{***}	(0.034)
ΔP_{t-2}	-0.143^{***}	(0.016)	-0.120^{**}	(0.027)
ΔP_{t-3}	-0.040^{***}	(0.012)	-0.043	(0.024)
$\Delta P_t^{(i-2)}$	0.015	(0.008)	-0.007	(0.008)
$\Delta P_t^{(i-1)}$	0.007	(0.009)	-0.020	(0.013)
$\Delta P_t^{(i+1)}$	0.018^{*}	(0.010)	0.045	(0.018)
$\Delta P_t^{(i+2)}$	0.001	(0.004)	0.020	(0.017)
P^{Auc}	0.004	(0.009)	-0.003	(0.014)
V_t	0.009	(0.007)	-0.015	(0.009)
Δw_t^n	-0.185	(0.295)	-2.401^{**}	(0.736)
Δw_t^p	-1.249^{*}	(0.632)	-2.795^{**}	(1.167)
Δs_t^n	-4.361^{**}	(1.654)	9.316^{***}	(1.459)
Δs_t^p	3.529	(3.289)	-11.441^{***}	(2.688)
Δt	0.011	(0.017)	0.021	(0.030)
#Obs	9032		1962	
R_{adj}^2	0.112		0.139	

H18Q4

Variable	Regime 1 $\xi \leq 0.632$		Regime 2 $\xi > 0.632$	
	Estimate	Std error	Estimate	Std error
Const	-0.915	(1.402)	-2.113	(2.030)
ξ	1.327	(2.497)	1.724	(3.016)
ΔP_{t-1}	-0.303^{***}	(0.023)	-0.334^{**}	(0.045)
ΔP_{t-2}	-0.152^{***}	(0.020)	-0.107	(0.032)
ΔP_{t-3}	-0.012	(0.017)	-0.081	(0.030)
$\Delta P_t^{(i-2)}$	0.000	(0.010)	-0.011	(0.011)
$\Delta P_t^{(i-1)}$	0.015	(0.010)	0.044	(0.011)
$\Delta P_t^{(i+1)}$	-0.007	(0.009)	0.008	(0.004)
$\Delta P_t^{(i+2)}$	0.000	(0.008)	0.011	(0.010)
P^{Auc}	0.005	(0.009)	0.013	(0.007)
V_t	0.000	(0.003)	0.003	(0.003)
Δw_t^n	-1.039	(0.697)	-2.175	(1.211)
Δw_t^p	-0.437	(1.036)	-0.227	(0.349)
Δs_t^n	0.518	(2.192)	0.410	(3.086)
Δs_t^p	-2.144	(1.708)	-5.344	(2.861)
Δt	-0.024	(0.020)	0.034	(0.021)
#Obs	5835		7270	
R_{adj}^2	0.113		0.134	

$^{*}p < 0.1$; $^{**}p < 0.05$; $^{***}p < 0.01$

Table 7: Estimation results of the extended fundamental model (2) for 15-minute contracts H18Q1–4.

regression model is used to examine how 15-minute intraday trading depends on the slope of the merit order curve.

Our estimation results reveal that autoregressive price changes up to the third order are highly statistically significant and negative, independent of the time of day. This behavior provides clear evidence of mean reversion in the price formation mechanism of 15-minute contracts. Additionally, price changes of neighboring contracts exhibit strong explanatory power and a positive impact on price changes of a given 15-minute contract. We observe an asymmetric effect of positive and negative renewable forecast changes on intraday prices depending on the merit-order-curve slope: Renewable forecasts affect electricity prices more severely in the steep than in the flat merit-order regime. In general, renewable forecast changes have a higher explanatory power for pricing noon than morning and evening contracts, but price information is the key driver of 15-minute intraday trading. Overall, we conclude that the importance of influencing factors on the intraday electricity market has changed from fundamental towards trade-related factors.

As our fundamental model exclusively involves *ex-ante* knowledge, it allows to develop trading strategies for intraday electricity markets, tailor-made for each contract. Furthermore, it helps to design forecasting models for single intraday transaction prices in the continuous trading – to our knowledge, an unexplored territory of scientific research hitherto. Moreover, our article provides a valuable step towards the optimization of the bidding behavior on intraday markets. Eventually, our insights should prove useful to energy companies within the process of automating intraday electricity trading.

Acknowledgements

Appendices

A Data

We provide a summary of explanatory variables, granularities, detailed descriptions and data sources in Table 8.

References

Burger, M., Klar, B., Müller, A., and Schindlmayr, G. (2004). A spot market model for pricing derivatives in electricity markets. *Quantitative Finance*, 4(1):109–122.

EPEX SPOT SE (2015). Press release: EPEX SPOT and ECC to reduce intraday lead time on all markets. `https://www.epexspot.com/document/32479/2015-06-16_EPEX%20SPOT_Lead%20time%20reduction_E-D-F.pdf`. (Accessed on Mar 1, 2019).

EPEX SPOT SE (2017). Press release: Exchange Council approves the introduction of 15-minute contracts on the Belgian and Dutch market – Trading until delivery to be launched

Variable [Unit] (*Granularity*)	**Description**	**Source**
Transaction price P_t [EUR/MWh] (*up to 1-minute*)	Transaction price of 15-minute contracts traded on the German continuous intraday power market at EPEX SPOT SE	European Energy Exchange AG (2016b)
Trading volume V_t [MW] (*up to 1-minute*)	Trading volume of 15-minute contracts traded on the German continuous intraday power market at EPEX SPOT SE	European Energy Exchange AG (2016b)
Auction price P^{Auc} [EUR/MWh] (*quarter-hourly*)	Market clearing price of 15-minute contracts traded in the German 15-minute intraday auction at EPEX SPOT SE	European Energy Exchange AG (2016c)
Wind power forecast w_t [GW] (*quarter-hourly*)	Intradaily updated forecast of wind power generation for each quarter-hour on the delivery day in Germany	EWE TRADING GmbH (2016)
Solar power forecast s_t [GW] (*quarter-hourly*)	Intradaily updated forecast of solar power generation for each quarter-hour on the delivery day in Germany	EWE TRADING GmbH (2016)
Expected demand l [GW] (*quarter-hourly*)	Day-ahead total load forecast for each quarter-hour on the delivery day in Germany (published: daily at 10 AM)	European Network of Transmission System Operators for Electricity Transparency Platform (2016)
Expected conventional capacity c [GW] (*daily*)	Expected daily average of available generation capacity of conventional power plants on the delivery day in Germany (published: daily at 10 AM)	European Energy Exchange AG Transparency Platform (2016)

Table 8: Summary of explanatory variables, granularities, detailed descriptions and data sources. Variables indexed by t vary over the continuous trading session of a given 15-minute contract.

on the German market on 14 June 2017. `https://www.epexspot.com/document/37626/170612_EPEX%20SPOT_Exchange%20Council.pdf`. (Accessed on Mar 1, 2019).

European Energy Exchange AG (2016a). EEX annual report 2015. `https://www.eex.com/blob/16500/ff13c25a4813320ff521bf67ac397e73/eex-gb-2015-en-data.pdf`. (Accessed on Mar 1, 2019).

European Energy Exchange AG (2016b). EPEX SPOT DE 15-minute intraday auction market data. `https://www.eex.com`.

European Energy Exchange AG (2016c). EPEX SPOT DE/AT 15-minute continuous intraday market transaction data. `https://www.eex.com`.

European Energy Exchange AG Transparency Platform (2016). Available generation capacity data. `https://www.eex-transparency.com`.

European Network of Transmission System Operators for Electricity Transparency Platform (2016). Day-ahead total load forecast data. `https://transparency.entsoe.eu`.

EWE TRADING GmbH (2016). Intradaily updated forecast data of wind and solar power generation. `https://www.ewe.com`.

Frauendorfer, K., Paraschiv, F., and Schürle, M. (2018). Cross-border effects on swiss electricity prices in the light of the energy transition. *Energies*, 11(9):2188.

Hansen, B. (2000). Sample splitting and threshold estimation. *Econometrica*, 68(3):575–603.

He, Y., Hildmann, M., Herzog, F., and Andersson, G. (2013). Modeling the merit order curve of the european energy exchange power market in germany. *IEEE Transactions on Power Systems*, 28(3):3155–3164.

Karakatsani, N. V. and Bunn, D. W. (2010). Fundamental and behavioural drivers of electricity price volatility. *Studies in Nonlinear Dynamics & Econometrics*, 14(4).

Kath, C. and Ziel, F. (2018). The value of forecasts: Quantifying the economic gains of accurate quarter-hourly electricity price forecasts. *Energy Economics*, 76:411–423.

Kiesel, R. and Paraschiv, F. (2017). Econometric analysis of 15-minute intraday electricity prices. *Energy Economics*, 64:77–90.

Märkle-Huß, J., Feuerriegel, S., and Neumann, D. (2018). Contract durations in the electricity market: Causal impact of 15 min trading on the EPEX SPOT market. *Energy Economics*, 69:367–378.

Pape, C., Hagemann, S., and Weber, C. (2016). Are fundamentals enough? Explaining price variations in the german day-ahead and intraday power market. *Energy Economics*, 54:376–387.

Paraschiv, F. (2013). Price dynamics in electricity markets. In Kovacevic, R., Pflug, G. C., and Vespucci, M. T., editors, *Handbook of Risk Management in Energy Production and Trading*, volume 199 of *International Series in Operations Research & Management Science*, pages 47–69. Springer Boston MA.

Wagner, T. (2018). emarketcrawlr: Crawling energy market data at EPEX SPOT (intraday trading, intraday auction, day-ahead auction). `https://github.com/wagnertimo/emarketcrawlR`. R package version 0.1.0.